

[CONTRIBUTION FROM PHYSICS LABORATORY, UNIVERSITY OF WISCONSIN]

## The Joule-Thomson Effect in Carbon Dioxide

By J. R. ROEBUCK, T. A. MURRELL AND E. E. MILLER

The Joule-Thomson effect has already been measured in air,<sup>1,2</sup> helium,<sup>3,4</sup> argon,<sup>5</sup> nitrogen,<sup>6</sup> in four mixtures of helium and nitrogen,<sup>7</sup> and in four mixtures of helium and argon.<sup>8</sup> The present article describes its measurement in carbon dioxide. For descriptions of general methods and apparatus reference is made to the above articles, particularly the air work. The changes in either methods or apparatus necessary for this special material are described below.

The general literature on the properties of carbon dioxide has been excellently summarized by Quinn and Jones.<sup>9</sup> This particular property of carbon dioxide has been discussed in much greater detail with many references by Burnett, both in a summary article<sup>10</sup> and in a very much detailed one.<sup>11</sup>

### Liquefaction

The compressor used in all the previous work served again here. It was provided with two interstage coolers fed with lake water. During the winter months this cooling water temperature was close to 1° and in summer it never exceeded the critical temperature, 31°. The delivery pressure for almost all the work exceeded the critical pressure. Hence the fluid sent to the apparatus was regularly liquid. If, to avoid this, the compressor operating temperature was raised above 31°, then much more of the lubricating water was carried forward as vapor leading to greatly increased trouble with the driers.

Thus operation at these temperatures gave a fairly incompressible liquid with considerable inertia through part of the cooling coils and on through the system. To avoid a dangerous rise of pressure on the delivery stroke a compression chamber was formed of a small steel cylinder, open end down, attached at a T in the line just following the delivery valve. This cylinder was immersed in water heated by a steam jet, so keeping the carbon dioxide in this cylinder well above its critical temperature. The rise of pressure on each delivery became quite tolerable.

In Burnett's work<sup>11</sup> no trouble had been experienced with any failure to separate in the water trap a denser liquid phase, mostly water, from a less dense phase, mostly carbon

dioxide. The necessary presence in our compressor of liquid water as a lubricant and as an agent for keeping the fiber packing swollen and soft, made the possibility of a phase denser than that of the (mostly) water one an important question. Since no such trouble had come to our attention, it was decided to go ahead till difficulty of some kind arose.

The piston rod of the compressor was bathed by the cooling water between two packed joints. The suction pressure in the first stage regularly fell below one atmosphere so that small amounts of water made their way into the system. No difficulty was experienced in purging this from the high pressure water trap. The purged froth changed abruptly to gas which was assumed, correctly, to indicate that the water was purged. It now appears that we might have encountered difficulty; see the work by Wiebe and Gaddy<sup>12</sup> and by Katz.<sup>13</sup> Our experience suggests a very small water concentration in the carbon dioxide liquid phase at 200 atm. pressure and temperatures between 10 and 25°, and a low concentration of carbon dioxide in the liquid water phase, with the water phase the denser and with no serious commingling of the phases.

For bath temperatures above 31° it was necessary to supply to the entering liquid carbon dioxide the large heat of vaporization. When 3 kw. of a. c. power proved inadequate, steam at 16 lb. gage pressure was used to heat the inflow liquid carbon dioxide after it had passed part of the inlet coil of the counter-current exchanger. The data for the temperatures from 50 to 300° were taken with this arrangement.

With the bath at 25° and the steam heating above omitted, violent trouble arose from the blocking by solid of the flow passages following the valve at which the pressure was reduced to atmospheric. This was avoided by steam heating the liquid before it passed this expansion valve. Since the return flow of the exchanger would carry only low pressure, it became necessary to build an exchanger where both flows could be at high pressure.

Fortunately the isenthalpic curves in the field below 25° all end at the vapor pressure curve so that for these measurements with liquid, return flows at pressures below the vapor pressure were not needed. Hence the return liquid carbon dioxide coming from the high pressure outlet coil of this exchanger was passed through a coil of copper pipe immersed in steam and then through a valve reducing its pressure to the inlet pressure of the compressor. This arrangement was used to take the data from 25° down in the liquid region.

For the region around the critical state and in the unsaturated vapor field, it was decided to discard the exchanger entirely since the bath would be close to room temperature. Part of the high pressure liquid carbon dioxide approaching the plug apparatus was passed through a coil immersed in a chamber filled with steam at 16 lbs.

(1) Roebuck, *Proc. Am. Acad. Arts Sci.*, **60**, 537 (1925).

(2) Roebuck, *ibid.*, **64**, 287 (1930).

(3) Roebuck and Osterberg, *Phys. Rev.*, **43**, 60 (1933).

(4) Roebuck and Osterberg, *ibid.*, **45**, 332 (1934).

(5) Roebuck and Osterberg, *ibid.*, **46**, 785 (1934).

(6) Roebuck and Osterberg, *ibid.*, **48**, 450 (1935).

(7) Roebuck and Osterberg, *THIS JOURNAL*, **60**, 341 (1938).

(8) Roebuck and Osterberg, *J. Chem. Phys.*, **8**, 627 (1940).

(9) Quinn and Jones, "Carbon Dioxide," Reinhold Pub. Corp., New York, N. Y., 1936.

(10) Burnett, *Phys. Rev.*, (2) **22**, 590 (1923).

(11) Burnett, *Bull. Univ. of Wisc.*, Vol. 9, No. 6 (1926).

(12) Wiebe and Gaddy, *THIS JOURNAL*, **62**, 815 (1940).

(13) Katz, *ibid.*, **62**, 1629 (1940).

per sq. in. gage, to supply the heat of vaporization of the carbon dioxide. The other part by-passed this heater. Valves in the two lines controlled the division so that the carbon dioxide could be sent into the apparatus at close to the bath temperature. A thermocouple with one junction in the bath and the other on the flow pipe close to its entry to the bath served to guide these valve settings.

It became immediately apparent that the reading of the inlet thermometer was quite sensitive to this adjustment. In the previous work we have adjusted the bath temperature, often at every point, to keep the inlet thermometer at the same reading. With this control of the temperature of inlet, adjustment of the bath became almost unnecessary and in the later plotting the initial point dropped sharply on its isenthalpic curve.

This very desirable result is to be attributed to two factors: (a) the smaller difference between entering fluid and bath allowing their better equalization, and (b) this in turn lessening the energy demand on the bath and so with the same stirring allowing greater uniformity of bath temperature. Similar improvement was noted in the past when some of the bath heating was shifted to the outside cylindrical wall and to the plug support. This supplied heat near the place of its loss, thus lessening the necessary heating of the bath fluid and so improving the uniformity of bath temperature. The adjustment of the entering fluid temperature to the bath temperature in the present case was so successful in avoiding the old difficulty—the first point falling off the curve—that a similar arrangement will be used whenever feasible. The erratic variation of the points was also much reduced and the isenthalpic curves in this group are as steady as any we have ever taken.

To prevent any possibility of the blocking again of the low pressure discharge by solid, the carbon dioxide coming from the plug was passed through the steam heater before expanding to one atmosphere. Since for part of the readings  $p_2$  would be followed down to a few atmospheres, a heater was built having large flow passages. For a number of points it became necessary to desert the automatic regulation of  $p_2$  and to depend on keeping the free piston of the  $p_2$  regulator floating by hand manipulation of this final expansion valve. At still more points it was sufficient to open the valve wide immediately following the automatic valve and to use this final expansion valve also to control the hunting of the regulator by limiting the pressure drop across the automatic valve.

This general situation of carbon dioxide liquefying or freezing has led to more experimental difficulty, more labor, and more variety of apparatus than any other material we have measured.

#### Carbon Dioxide Supply

The carbon dioxide used in this work was purchased from the Liquid Carbonic Corporation, usually in 50-lb. cylinders. For the earlier work, with the bath above room temperature, they selected for us cylinders filled at a time of minimum air impurity.

For the work well above the critical temperature excessive purity was not very important. As received, the air impurity, measured in the vapor phase, was around 0.1% by volume. During the work air entered the low

pressure system slowly and carbon dioxide was lost from the high pressure system also slowly. The higher purity of the carbon dioxide replaced from the liquid phase was more than offset by the entering air, and the purity fell gradually to 0.5 or 0.6%. For this part of the field the error from this impurity probably did not exceed the other errors of the measurements.

But in the neighborhood of the vapor pressure curve and indeed generally in the liquid phase, air impurity has a marked effect on the data. Small scale experiments showed immediately that freezing the liquid carbon dioxide slowly by means of liquid air forced almost all the air impurity into the vapor phase. A second freezing of a 100-g. sample normally yielded so little non-condensable impurity as to be difficult to determine.

The contents of a 50-lb. cylinder were transferred to our own cylinder. This cylinder was stood in a tall narrow metal vessel, and solid carbon dioxide, "dry-ice," packed around it first at the lower end. Gradually the dry-ice was filled in until it covered the cylinder. The outside was protected by cotton wadding and paper. Next morning the pressure in the cylinder was down to only a little above one atmosphere. The vapor was then allowed to blow off until the air in the escaping vapor was 0.1 to 0.01 vol. %. With slow freezing and not too cramped vapor space, the remaining air impurity in the vapor phase with the cylinder back at room temperature was below 0.01%.

To make effective use of such purity this complicated system had to be exceedingly free from leaks. Some six weeks was spent eliminating leaks, with such effect that during the taking of the data about the saturation curve the impurity increased from 0.01% to only 0.1%. These analyses were made on the vapor phase, which always carries relatively more air impurity, while the liquid contains the major part of the mass of the carbon dioxide. A few analyses were made of samples collected from the flow during a run without showing anything unexpected.

Since the carbon dioxide was made by combustion of coal or coke, it might contain some sulfur dioxide. None could be found in the spent potassium hydroxide used in some of the analyses.

E. S. Burnett<sup>11</sup> and the senior author had concluded about 1910 that the course of the curves in the liquid region approaching the vapor pressure curve was markedly influenced by the presence of volatile impurity. At that time the curves carrying sometimes as much as 1.5% air, were bent down to run below and nearly parallel to the vapor pressure curve. In the present work, it is shown experimentally that sufficiently pure carbon dioxide gives curves in this region which enter the vapor pressure curve without observable change of curvature (see Figs. 2 and 3). To investigate further the effect of air impurity, curves were now run with fluids containing different proportions of air impurity. Each separate point in one run requires its own  $p_2$  which has to be obtained by changing the amount of carbon dioxide in the flow system. Since the air impurity does not divide proportionately to the masses of the liquid and vapor phases, changes of the mass in the flow system always alter the proportion of volatile impurity. The curves of Fig. 1 thus show only qualitatively the effect of air impurity, since the impurities indicated there do not hold precisely for all the points. The propor-

tion of air impurity generally decreases somewhat toward the lower pressures.

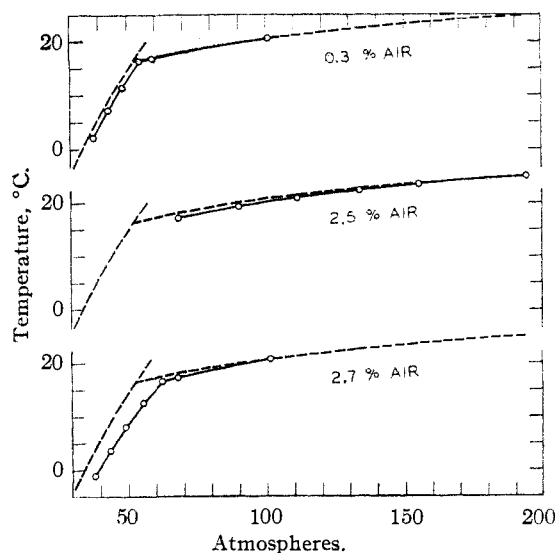


Fig. 1.—Isenthalpic curves showing the effect of volatile impurity.

One can, nevertheless, observe that as the curve approaches the saturation curve it bends discontinuously to run down beside the saturation curve and approach it slowly. The larger the impurity, the farther from the saturation curve the break occurs, and the more rapidly the new branch approaches the saturation curve. The general behavior of liquid and vapor suggests that the volatile impurity should break the continuity of the liquid, that is, form bubbles of vapor, at a somewhat higher pressure than the vapor pressure of the pure liquid and the rise above this vapor pressure should increase with increase of volatile impurity. Also as the volume of the vapor phase grows, the proportion of volatile impurity therein decreases, and the shift from the vapor pressure correspondingly decreases.

In Fig. 1 the dashed line with each run is a corresponding run made with fluid having negligible volatile impurity. It will also be observed, but not readily predicted, that the curve for the liquid carrying volatile impurity has a steeper slope than for that of the pure liquid ( $\mu$  is increased) and that this increase grows with impurity and also somewhat with approach to the saturation curve. Little or nothing is known about the Joule-Thomson effect in mixtures near the saturation conditions of one component. Such measurements offer great difficulty in the control of the composition.

**Piston Gage.**—During the gathering of the Joule-Thomson data there was observed a uniform difference of 3 to 4% between our new vapor pressure data and those of Meyers and Van Dusen, very suggestive of an error in the pressure scale. The open-tube mercury manometer<sup>14</sup> was used in 1937 to measure the vapor pressure of carbon dioxide at the ice point and the observed value is very close to the data in the literature. To check up on the scale of the piston manometer, it was used to measure the

same vapor pressure. This same discrepancy of 3–4% appeared.

The scale of the piston manometer had been set originally in 1912 by micrometer measurement of the piston diameter, and by the simultaneous measurement of a pressure with the piston manometer and with an open-tube mercury manometer. The two methods agreed to slightly under 0.1%. These data were now re-examined and an arithmetical error found in the factor used for transferring load readings into atmospheres. This factor as used in later work is 1.457, while from the 1912 data it should have been 1.404. The factor as measured now from the ice-point work is 1.410, a difference of 0.4%.

This change is small enough to be of little importance in its effects on the data already taken with this gage. For, first, we have not found it possible to get consistently with the gage pressure readings during flow better than about 0.1 lb. load or 0.15 atm., and we consistently record only to 0.1 lb. load. To read the pressure in a stationary system is a quite different problem. Second,  $\mu$  is a slow function of the pressure except in the critical state and low-pressure unsaturated-vapor regions, so the absolute value of the pressure is generally not very critical. Third, a uniform drift totaling 0.4% in twenty-six years could hardly affect the values of  $\mu$  calculated from successive readings and a sudden change would affect very few values. The effects of heat leaks and regulatory uncertainties in both pressure and temperature are much more serious. Hence in correcting earlier work for pressure scale errors we are correcting only the numerical mistake.

With the exception of the two last published articles,<sup>8,15</sup> all the work from this Laboratory on the Joule-Thomson effect must be corrected for this error in the pressure scale. The numbers representing pressure have to be multiplied by 0.9677 to express them correctly in atmospheres. Suitable corrections must also be made in the derived quantities like  $\mu$ . These corrections have been made to the data in this article.

The open-tube manometer<sup>16</sup> is being revised and is not available for calibrating the piston manometer except as above through the ice-point readings of the vapor pressure. The only available confirmation appeared to be to read the vapor pressure at a series of temperatures and compare the results with Meyers and Van Dusen's data. Table I, Column 1 gives the chosen temperatures, Col. 2 the piston manometer readings of the vapor pressure, and Col. 3 the interpolated data from Meyers and Van Dusen.<sup>17</sup> The maximum difference between the pairs of readings is 0.05%.

Hence both from our mercury manometer readings and from the Meyers and Van Dusen comparison, our piston-manometer scale is now correct to a small fraction of 1%.

**Isenthalpic Curves.**—The data from the first group of measurements are given in Table II. The individual runs are referred to by their approximate bath temperature. The last temperature and pressure in a run are, respectively,

(15) "Temperature. Its Measurement and Control in Science and Industry," Reinhold Pub. Corp., New York, N. Y., 1941, pp. 60–73.

(16) Roebuck and Miller, *Rev. Sci. Instr.*, **10**, 179 (1939).

(17) Meyers and Van Dusen, *Bur. Standards J. of Res.*, **10**, 381 (1933).

(14) Roebuck and Cram, *Rev. Sci. Instr.*, **8**, 215 (1937).

the bath temperature and the inlet high pres-

sure. The temperatures are in the hydrogen centigrade scale and the pressures in atmospheres absolute.

A few of the runs were repeated to be assured occasionally that the data did not depend on the rate of flow or the particular plug. The reliability of apparatus and methods have been sufficiently proved in the previous work. It would appear that the uniformity with which the points fall on a curve, and the consistency of the family of

TABLE I  
VAPOR PRESSURES (COLUMN 2) AS READ AT WISCONSIN AND (COLUMN 3) AS INTERPOLATED FROM MEYERS AND VAN DUSEN<sup>17</sup>

<i>t</i> , °C.	<i>p</i> , atm.	<i>p</i> , atm.
28.51	68.79	68.799
23.64	61.50	61.529
20.19	56.78	56.779
14.76	49.93	49.905
0.0	34.41	34.397

TABLE II

EXPERIMENTAL DATA FOR ISENTHALPIC CURVES OF FIG. 2

No.	<i>p</i>	<i>t</i>	No.	<i>p</i>	<i>t</i>	No.	<i>p</i>	<i>t</i>	No.	<i>p</i>	<i>t</i>			
300° curve, Plug 11			150° curve, Plug 14			76° curve, Plug 43			50° curve, Plug 43			0° curve, Plug 11		
1	3.1	258.37	1	4.6	47.04	6	87.7	44.39	1	111.6	39.54	1	32.1	-2.73
2	19.3	263.16	2	19.5	60.77	7	111.5	58.40	2	132.1	42.77	2	37.7	-2.42
3	41.0	268.68	3	43.2	79.25	8	131.8	67.40	3	155.0	45.56	3	49.4	-2.05
4	64.0	274.25	4	66.6	94.95	9	155.2	75.42	4	193.5	49.26	4	69.1	-1.47
5	87.7	279.55	5	90.5	108.35	10	193.5	85.36	5	89.6	-1.05			
6	109.4	284.44	6	112.5	119.45	1	41.1	6.65	6	112.0	-0.63			
7	131.5	288.60	7	134.8	129.09	2	64.4	25.18	7	133.7	-0.39			
8	193.5	299.53	8	155.5	136.59	3	86.7	40.37	8	155.8	-0.20			
250° curve, Plug 14			125° curve, Plug 1			50° curve, Plug 43			-25° curve, Plug 11					
1	89.7	226.01	1	64.3	61.62	4	110.8	53.18	1	54.0	17.80	1	23.8	-24.38
2	113.3	232.25	2	88.0	78.44	5	131.9	61.18	2	65.1	25.70	2	31.7	-24.23
3	133.8	237.48	3	109.3	91.43	6	155.0	67.87	3	76.6	31.21	3	44.7	-24.30
4	156.2	242.72	4	131.5	102.33	7	193.5	76.47	4	87.5	34.36	4	67.6	-24.32
5	194.7	250.69	5	155.0	112.20	75° curve, Plug 43			5	111.6	39.51	5	89.6	-24.37
250° curve, Plug 11			125° curve, Plug 43			1	41.1	7.04	37° curve, Plug 11			6	112.9	-24.47
1	2.5	197.49	1	2.5	-0.94	2	52.2	16.62	1	56.5	19.85	7	133.5	-24.60
2	19.7	203.71	2	24.7	+25.78	3	65.1	26.12	2	59.3	21.95	8	155.3	-24.72
3	44.3	211.84	3	46.2	47.26	4	76.5	33.90	3	60.8	22.87	9	194.4	-25.37
4	68.2	219.21	4	70.4	67.24	5	87.4	40.73	4	62.6	23.71	-38° curve, Plug 61		
5	91.2	226.20	5	93.2	82.60	6	111.8	52.93	5	65.4	24.20	1	11.6	-36.94
6	112.6	231.82	6	193.5	125.09	7	132.4	60.30	6	68.6	24.81	2	13.2	-36.96
7	134.9	237.45	100° curve, Plug 43			8	155.6	66.75	7	74.0	25.66	3	15.6	-36.97
8	193.5	250.56	1	1.9	-61.60	9	193.5	74.63	8	85.2	27.40	4	23.3	-37.01
200° curve, Plug 14			2	22.5	-15.30	74° curve, Plug 43			9	106.3	30.05	5	33.5	-37.11
1	3.8	128.90	3	41.1	+8.22	1	41.0	6.54	10	128.3	32.07	6	59.1	-37.37
2	19.5	137.19	4	64.4	34.05	2	58.9	21.05	11	155.5	34.16	7	97.7	-37.79
3	43.5	148.78	5	86.2	52.66	3	65.1	25.52	12	194.4	36.51	-50° curve, Plug 11		
4	64.8	158.08	6	110.8	68.22	4	72.2	30.04	25° curve, Plug 55			1	33.7	-47.67
5	88.4	167.62	7	132.2	78.91	5	88.3	40.59	1	88.7	19.77	2	44.2	-47.91
6	113.1	176.65	8	155.0	88.15	6	111.8	52.32	2	111.8	21.39	3	66.6	-48.26
7	133.5	183.46	9	193.5	100.03	7	132.4	59.86	3	134.4	22.59	4	89.9	-48.49
8	156.2	190.33	85° curve, Plug 43			8	155.0	66.19	4	193.7	25.02	5	111.4	-48.90
9	194.7	200.48	1	20.5	-17.43	9	193.5	74.28	25° curve, Plug 11			6	133.9	-49.19
150° curve, Plug 55			2	31.8	-2.77	74° curve, Plug 61			1	55.4	16.74	7	155.3	-49.46
1	89.9	108.52	3	42.4	+8.29	1	59.7	21.57	2	62.3	17.40	8	194.4	-50.74
2	113.0	120.07	4	54.4	18.36	2	63.0	23.93	3	69.1	18.18	-50° curve, Plug 61		
3	134.2	129.45	5	65.5	26.65	3	66.1	25.86	4	90.4	19.99	1	10.8	-47.32
4	155.8	137.49				4	68.9	27.76	5	113.5	21.50	2	13.0	-47.35
5	194.7	149.74				5	84.3	38.41	6	135.4	22.70	3	20.3	-47.43
						6	100.7	47.62	7	194.4	25.02	4	31.9	-47.57
						7	134.9	60.48				5	56.1	-47.83
												6	97.7	-48.57

curves and of the family of their derivatives, give sufficient assurance of the reliability of the data.

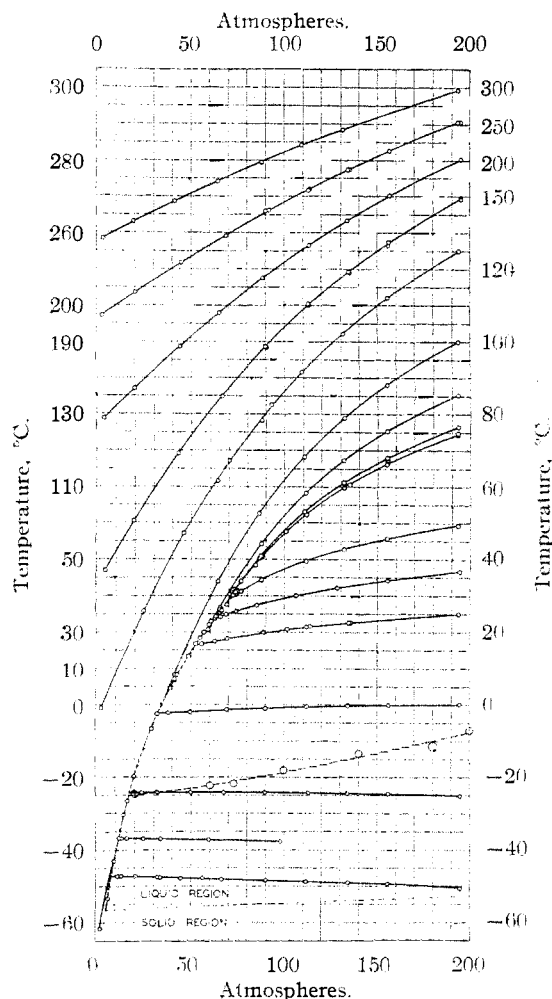


Fig. 2.— $t$  as a function of  $p$  at constant enthalpy, over the whole field.

The data of Table II are plotted in Fig. 2, with temperature as ordinate and pressure as abscissa. The pressure scale is unbroken, but the temperature scale is broken and the upper temperature curves are crowded together. This is not feasible in the liquid-vapor region.

It will be observed that the points fall on the curves in Fig. 2 a little less consistently than, for example, in the nitrogen<sup>6</sup> or argon<sup>5</sup> articles. The constant presence of liquid and vapor coming from the compressor, and the large quantity of heat to be added, definitely increased the difficulty of both fine pressure and fine temperature regulation. Slight drifts and irregularities in these controls are very serious in their effect on the regularity of the data. It may be that such ir-

regularities are largely smoothed out in the final treatment of the data, but one is much better satisfied where such smoothing is at a minimum. It was not large here, though somewhat larger than in much of the earlier work.

The general form of the family of these isenthalpic curves is the same as with all the pure substances and mixtures we have measured. With falling bath temperature the curves increase in slope and curvature, (a) below the critical pressure to the lowest temperature measured, and (b) above the critical pressure this trend reverses some distance above the critical temperature. The rate of decrease of slope with falling temperature rises to a maximum along the 200 atm. ordinate at perhaps  $60^\circ$  and falls again to a quite low rate in the liquid region where the slope finally becomes negative and the curves nearly straight. The maximum rate occurs in those curves entering the vapor pressure curve in the neighborhood of the critical point, and right at the critical point this rate becomes infinite.

At the highest pressure and a little below the critical temperature maxima appear on the isenthalps and these maxima shift to the left with falling temperature until they disappear into the vapor pressure curve. The locus of these maxima, called the "inversion curve," is plotted in Figs. 2 and 3.

In the unsaturated vapor region the slope continues to grow with falling temperature till the curves disappear either into the vapor pressure curve or into the zero pressure ordinate. The  $100^\circ$  curve has its lowest point off the vapor pressure curve, in the unsaturated vapor region below the triple point at about  $-62^\circ$ . An actual difference of temperature across the plug of 160° was observed, which exceeds the largest previously observed,<sup>5</sup> namely, that for argon, of  $120^\circ$ . The corresponding maximum slope for carbon dioxide is  $\mu = 2.8^\circ/\text{atm.}$  while for argon<sup>6</sup> it is  $3.0^\circ/\text{atm.}$

The curves above room temperature were measured first. As the curves running into the critical region were measured, great difficulty was experienced in obtaining consistency in their approach to the neighborhood of  $T_c p_c$ . The difficulty was immediately traced to the presence of small air impurity. As described above this was solved by freezing the liquid and blowing off sufficient of the overlying vapor. The curves about  $T_c p_c$  were not repeated exactly and the best are

plotted in Fig. 2, where they show more than desirable inconsistency near  $T_c p_c$ . They are supplemented by a whole new group of curves, Fig. 3, described below, covering the  $T_c p_c$  region. But first the set of curves, Fig. 2, in the liquid region was measured, using the purer carbon dioxide. The field was covered down to the solid-liquid line, the slope there becoming quite markedly negative. This last curve involved some thrill for the experimenters, since a small failure of the controls could have blocked the flow passages with solid. The curves were followed close to the saturation curve to be sure that the steady slope and curvature persisted right to the saturation curve. In Figs. 2 and 3 are given carefully measured curves well down in the liquid region, having points close to the entry into the vapor pressure curve. These curves thus give positive evidence that the inversion curve does not bend down in the liquid region but disappears directly into the saturation curve. This form of the inversion curve with the turn down, coming originally from an equation of state, is thus definitely excluded for carbon dioxide by this experimental evidence.

**Vapor Pressure Curve.**—The saturation curve is plotted in Fig. 2 as a dashed line through the points measured when a mixture of liquid and vapor is escaping from the plug wall. These points scatter along the curve very similarly to the regular points along the isenthalpic curves. Very few of the total number of points can be shown in Fig. 2. A set of values read from this dashed curve is given in Column 2 of Table III. A corresponding set from the original drawing of Fig. 3 is given in Column 3. These two sets from entirely independent data are in reasonable agree-

TABLE III

## VAPOR PRESSURE OF CARBON DIOXIDE

Column 2 is from the data of Fig. 2. Column 3 from that of Fig. 3. Column 4 is the weighted average of 2 and 3. Column 5 is the corresponding data from Meyers and Van Dusen.<sup>17</sup>

$t$ , °C.	$p$ , atm.	$p$ , atm.	$p$ , atm.	$p$ , atm.
31	72.6	72.7	72.7	72.8
30	70.9	71.2	71.1	71.2
20	56.3	56.8	56.6	56.5
10	44.3	44.4	44.4	44.4
0	34.5	34.2	34.3	34.4
-10	25.9	26.0	26.0	26.2
-20	19.1	19.5	19.4	19.5
-30	13.6	14.1	13.9	14.1
-40	9.6	10.0	9.9	9.9
-50	6.8	6.7	6.7	7.0

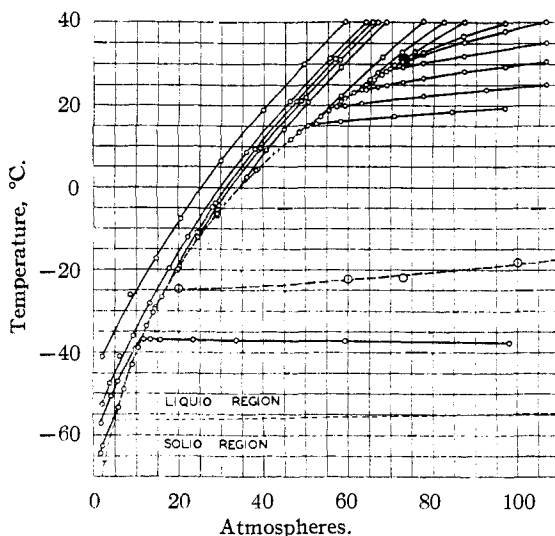


Fig. 3.— $t$  as a function of  $p$  at constant enthalpy, in the neighborhood of the saturation curve.

ment. The averages are given in Column 4, giving twice the weight to Column 3 on account of its better experimental conditions. The last readings in Columns 2 and 3 depend on too few data taken under the most difficult of the experimental conditions. For comparison the vapor pressures measured by Meyers and Van Dusen<sup>17</sup> are given in Column 5. The agreement within 1% is as much as one can expect under the difficult conditions of the flow measurements.

That the presence of air impurity in the carbon dioxide is not exerting a measurable influence on these vapor pressure readings is shown *first* by the close check between the values determined statically (Col. 5) and those determined dynamically (Col. 4); and *second* by the precision with which points on the vapor pressure curve coming from the extension of curves from the liquid region and from the unsaturated vapor region fall together on one common curve. These two series of points will have quite different proportions of liquid and vapor, and the effects of a volatile impurity will necessarily depend on this proportion.

In a new plotting of his experimental data, kindly made for us by E. S. Burnett,<sup>11</sup> all his saturation points fall below Meyers and Van Dusen's vapor pressure curve. Burnett's fluid carried around one volume per cent. of air, so that the curves entering from opposite sides of the vapor pressure curve give saturation points spread over a band of definite width. The air impurity disturbs the saturation points of curves entering from

the unsaturated vapor side, less than those from the liquid side. Whatever effect there is on the latter may be expected to move these saturation points toward the liquid region from their location when undisturbed by impurity. We consider this disturbance as probably unimportant for the saturation points on curves from the vapor side.

One now may well ask whether the two ways of reading the vapor pressure—that is, (a) a static method using a liquid at rest in a vessel except for possible gentle stirring, and (b) a dynamic method where the mixed liquid and vapor are rushing through passages—actually lead to different values. Burnett<sup>11</sup> (p. 87) points out that if the vapor condenses during its passage through the plug, the droplets formed will be very small and will be kept small by the turbulence. So that while passing the thermometer the droplets might still be very small and have the higher vapor pressure associated with the steep convexity of the liquid-vapor surface. This would account for a vapor pressure of the vapor-rich mixture being higher than in the measurements of bulk liquid. Since the surface tension goes to zero at the critical temperature, this effect must also vanish there, even though it might be favored in this neighborhood by more ready divisibility of the liquid droplets. This situation can occur only in the saturation points following along a curve from the unsaturated vapor region—that is, from above—since only in these will the proportion of liquid present be small.

For the curves coming into the vapor pressure curve from the liquid side, the liquid disrupts to form a bubble of vapor only after the pressure has fallen somewhat below the actual vapor pressure of the liquid at its prevailing temperature. If the pressure is under outside control, the temperature adjusts itself through evaporation, to fit on the bulk vapor pressure curve. The retarding effect of the surface tension on the formation of a bubble will be reduced by the violent turbulence and rough surfaces in the plug.

Since the groups of points associated with the two regions fall well on a common curve, we may conclude that the effects of surface tension are not of moment in this situation.

One can also say that this practical identity of the two sets of points excludes hypotheses as to the failure to reach equilibrium among molecular species in the short time allowed in the flow experiments. This is also excluded by the inde-

pendence of the values on the size of the flow through the plug.

### Conditions Near the Vapor Pressure Curve

To search out the experimental situation about  $T_c p_c$  and the vapor pressure curve generally, a second series of experiments was carried out. The data are given in Table IV and are plotted in Fig. 3 with the same temperature scale but twice the pressure scale of Fig. 2. The bath was held at 40° while the initial pressure was set successively at a series of values between 59 and 106 atm., and the curves followed to the saturation curve and often along it. To avoid confusion only a part of the points taken along the saturation curve are plotted in Fig. 3, though they were plotted and used in the original drawing from which Fig. 3 was traced. The series was completed by holding the inlet pressure at 106 atm. while using a lower bath temperature in each successive run. These curves supplied still more saturation curve points.

This series of curves examines the manner of entry of the isenthalpic curves into the vapor pressure curve of the liquid, from both sides, all the way from the critical state to the triple point. The curves of Fig. 2 in the liquid region somewhat below the critical state were also taken with air-free material and serve to fill in this region in Fig. 3.

The series of Fig. 3 was begun with an air impurity in the carbon dioxide, measured in the vapor phase, of less than 0.01 volume per cent. At the end of the series this had risen to 0.12% again as measured in the vapor phase. Both measurements had to be made at times flow readings were not in progress, as during flow the situation is already sufficiently complex. It consequently seems safe to say that the actual air impurity carried by the flowing material was distinctly below the above values. There was no evidence observed, either in the data or in the curves resulting, of the presence of volatile impurity.

The curves of Fig. 3 were measured in the following order: first, those about  $T_c p_c$ ; and second, those in the unsaturated vapor region on the low pressure side of the vapor pressure curve. Since the effect of air impurity is much more marked around  $T_c p_c$ , this region was measured first with the high initial purity.

The conditions during the measurements in-

TABLE IV  
 EXPERIMENTAL DATA FOR ISENTHALPIC CURVES OF FIG. 3

No.	$p$	$t$	No.	$p$	$t$	No.	$p$	$t$	No.	$p$	$t$
40°, 59 atm. curve, Plug 65			40°, 67 atm. curve, Plug 65			40°, 82 atm. curve, Plug 61			35°, 106 atm. curve, Plug 61		
1	1.9	-41.17	1	7.0	-48.97	1	59.0	21.74	1	64.0	25.06
2	8.4	-28.18	2	10.2	-39.03	2	61.0	23.14	2	65.8	26.61
3	14.5	-17.30	3	13.9	-30.46	3	62.9	24.50	3	68.7	28.40
4	20.2	-7.73	4	19.3	-20.23	4	64.7	26.30	4	70.6	28.69
5	30.0	+6.49	5	24.3	-12.27	5	66.8	28.04	5	72.6	29.15
6	39.7	18.94	6	29.4	-4.52	6	72.5	32.94	6	77.4	30.27
7	49.4	30.03	7	39.3	+9.48	7	82.3	40.00	7	87.1	31.87
8	59.0	40.00	8	48.7	21.14				8	106.4	35.02
40°, 64 atm. curve, Plug 65			40°, 69 atm. curve, Plug 65			40°, 87 atm. curve, Plug 61			30°, 106 atm. curve, Plug 65		
1	1.9	-52.63	1	2.0	-62.63	1	29.0	-6.42	1	63.9	23.94
2	3.8	-47.48	2	15.9	-26.61	2	38.7	+4.47	2	66.7	24.60
3	5.9	-42.94	3	20.0	-19.32	3	48.5	13.28	3	68.7	24.93
4	9.2	-36.19	4	28.9	-6.50	4	58.1	21.07	4	72.6	25.65
5	13.1	-28.23	5	36.1	+2.32	5	65.8	26.27	5	77.4	26.67
6	17.6	-19.69	6	44.9	14.09	6	70.6	29.34	6	87.1	28.17
7	22.0	-12.09	7	68.7	40.00	7	75.6	33.04	7	96.7	29.39
8	27.9	-2.86				8	87.1	40.00	8	106.4	30.55
9	36.0	+8.56	40°, 69 atm. curve, Plug 65			40°, 97 atm. curve, Plug 61			25°, 106 atm. curve, Plug 65		
10	46.1	21.11	1	1.5	-64.51	1	61.0	23.17	1	53.2	17.29
11	55.4	31.38	2	5.8	-53.53	2	65.7	26.40	2	55.2	18.68
12	63.9	40.00	3	8.9	-43.16	3	69.7	29.03	3	57.1	19.61
40°, 66 atm. curve, Plug 65			4	12.2	-33.77	4	72.5	30.55	4	59.0	19.91
1	1.6	-57.30	5	40.6	+8.95	5	77.4	32.77	5	62.9	20.48
2	4.0	-50.71	6	50.3	20.79	6	87.0	36.61	6	77.4	22.28
3	5.6	-47.16	7	58.2	29.25	7	96.8	39.79	7	92.2	23.81
4	9.6	-39.26	8	68.7	40.00	40°, 106 atm. curve, Plug 61			8	106.4	25.00
5	14.4	-29.26	40°, 77 atm. curve, Plug 61			1	62.9	24.00	19°, 97 atm. curve, Plug 65		
6	19.7	-19.15	1	19.6	-19.87	2	65.3	25.87	1	46.4	11.59
7	24.2	-10.97	2	28.7	-6.76	3	67.6	27.54	2	48.4	13.29
8	28.7	3.82	3	38.3	+4.26	4	70.3	29.15	3	50.4	14.97
9	38.0	+9.36	4	48.4	13.55	5	72.6	30.45	4	52.3	15.43
10	47.6	21.11	5	58.1	22.21	6	77.4	32.32	5	58.1	16.04
11	56.7	31.22	6	67.8	31.80	7	87.1	35.27	6	70.6	17.21
12	65.5	40.00	7	77.4	40.19	8	96.7	37.88	7	84.2	18.41
40°, 67 atm. curve, Plug 65						9	106.4	40.00	8	96.8	19.25
1	38.9	9.10									
2	49.7	22.03									
3	57.9	31.07									
4	66.8	40.00									

volved in Fig. 3 were decidedly better than in those of Fig. 2. This may be attributed to (a) the lower maximum pressure, (b) the proximity of the bath temperature to room temperature, and (c) the more effective use of the steam heating, particularly the arrangement by which the fluid entered the plug apparatus close to this apparatus temperature. It will be noted how well the points fall on the curves.

The uncertainty noted above about  $T_c p_c$  in Fig. 2 is no longer present. The curves enter the vapor pressure curve from either side without any change in their steady curvature, and enter it so as to make a consistent family. The vapor pres-

sure curve drawn through the sets of points coming from above and from below shows no larger spread than each group within itself. In the earlier work, for example, with air<sup>2</sup> and with nitrogen<sup>6</sup> this was also the case, but the great distance of the bath from room temperature made its temperature control much less certain, and the gathering of adequate data very expensive in time and in labor. In the case of argon<sup>5</sup> this condition was not as well satisfied and the present work confirms the inference made then that it was to be attributed to the presence as impurity of the more volatile nitrogen.

In the first group of curves plotted in Fig. 2



the 100° curve runs into the saturation curve, and after a number of points along it, comes off from it into the unsaturated vapor region again. This requires that during the measurement of one of these lower points the carbon dioxide in its passage through the wall of the porcelain plug began to condense to liquid, the proportion of liquid increased to a maximum, decreased, and disappeared before the fluid emerged again from the wall. This phenomenon appears again in a number of the curves of Fig. 3. Burnett<sup>11</sup> (p. 34) refers to the high probability of such a situation in carbon dioxide but lacked the means to realize it experimentally.

The group of curves in Figs. 2 and 3 actually cutting the vapor pressure curve or passing close above it, allow of fixing the tangent point at which a particular one of these isenthalpic curves touches the vapor pressure curve. The point of tangency determined from the data in Fig. 3 lies close to 13.8 atm. and  $-30.6^\circ$ . The data of Fig. 2 would place it nearer to  $-20^\circ$  but here the entry and exit points are much more widely separated, the air impurity is probably larger, and the confirmation from neighboring curves practically absent. The point from Fig. 3 is definitely preferable. This point of tangency is about  $6^\circ$  above the point where the inversion curve enters the vapor pressure curve from the liquid side.

It will also be observed that these curves near both their entrance and their emergence become more widely separated from their nearly parallel neighboring curves. Since these are constant enthalpy curves, this means that the rate of change of enthalpy with distance, measured normal to these curves, decreases. One might expect that approaching the vapor pressure curve the unsaturated vapor would carry an increasing quantity of molecular complexes—possibly of the nature of small liquid droplets. Both increased pressure and decreased temperature might be expected to facilitate their formation. These would normally evolve heat in their formation, so increasing  $C$  and making the constant enthalpy curves move closer together. Actually the curves move apart so that only complexes which absorb heat in their formation can answer the requirements. These could not be liquid-like since all liquids give out heat in formation from their vapors. This would thus seem to be evidence against the increase of association in carbon dioxide vapor approaching its saturated condition.

The steady course of the isenthalpic curves in the liquid region right up to the vapor pressure curve affords evidence against any changes in the liquid depending on the nearness to the vapor equilibrium. Thus, speaking figuratively, there is no anticipation in the liquid of the approach of the vapor-liquid equilibrium. There seems to be a slight amount of anticipation in the vapor.

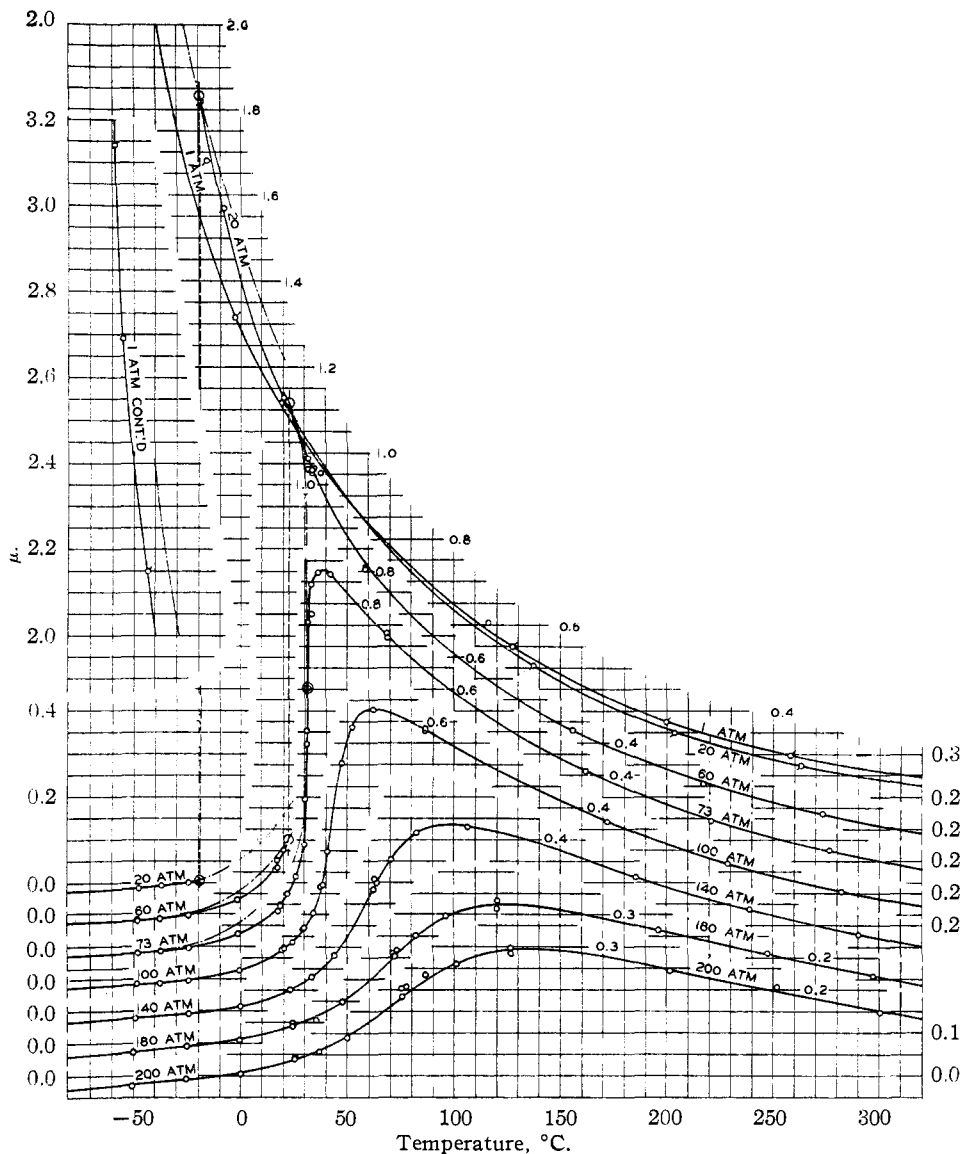
In Fig. 3 if one starts at  $T_c p_c$  and moves down parallel to, above, and very close to the curve—that is, in dry saturated vapor—one crosses constant enthalpy curves of progressively higher enthalpy—that is, on this path the enthalpy is increasing—until one reaches this point of tangency. From here on the opposite situation holds, the enthalpy on this path is now decreasing. Hence along this path the enthalpy is a maximum at this point of tangency. This maximum of the enthalpy is discussed by Plank and Kuprianoff<sup>18</sup> who locate it at about  $-20^\circ$  on the basis of earlier work. Burnett's<sup>11</sup> Chart IX places it about  $-26^\circ$ , while above we place it at  $-30.6^\circ$ .

**Joule-Thomson Coefficient,  $\mu \equiv (dt/dp)_h$ .**—As in previous papers<sup>1,6</sup> the numerical values of  $\mu$  are obtained by taking the ratio of the successive and corresponding differences of temperature and pressure for each experimental run. These values of  $\mu$  are plotted against the corresponding average pressure to give a set of isenthalpic curves. From each of these curves successive differences between  $\mu$ 's for a constant arbitrary interval in  $p$  are plotted against the average  $p$  for its interval. Adjustment between these curves served to smooth  $\mu$  as a function of  $p$ , and aid the choice of a satisfactory representative curve for  $\mu = f(p)_h$ .

From these smoothed curves the values of  $\mu$  for a series of selected pressures were read off. The temperature corresponding to each value was then read from the curves of Fig. 2 or 3. These data are plotted to give the curves of Fig. 4. This cross plotting was used to make further small adjustments between experimental points and curves drawn through them in the  $\mu = f(p)_h$  group. This places all the smoothing at one place in the reduction process where its size and character can be appreciated and controlled.

The general character of Fig. 4 bears the usual close similarity to that of every other substance except helium we have measured. It is again necessary to break the  $\mu$  scale to avoid having

(18) Plank and Kuprianoff, *Z. ges. Kälte-Industrie*, **36**, 41 (1929).

Fig. 4.— $\mu$  as a function of  $t$  at constant pressure.

the curves become indistinguishable at each end. This confuses the use of Fig. 4 for the consideration of relations among the curves. As with the other substances, the curves for low pressure, e. g. 1, 20, and 60 atm. in the case of carbon dioxide, cross each other and rise to the limit curve. The crossing here is more obvious than usual and the rise has been followed farther. It will be noted that a section of the 1 atm. curve has been moved out of its regular place.

The pressure range covered by the readings (1–200 atm.) is the same as in most of our preceding work. The temperature range has been somewhat restricted at the low end of the scale by the freez-

ing of the liquid. In terms, however, of the corresponding state variables, the range of the measurements is the smallest we have yet presented, due to the large values of  $T_c$  °K. and  $p_c$  atm. in carbon dioxide. It is the first material in which we have been able to extend our measurements over the whole temperature range of the liquid state, and to examine experimentally the situation in the vapor region and particularly about the critical point with considerable care.

The locus of the cutting points of the isenthalps of Figs. 2 and 3 with the vapor pressure curve, when plotted in terms of  $\mu$  and  $t$  appear in Fig. 4 as the "vapor and liquid limit" curves plotted as

dash-dot lines. The vertical dashed lines of Fig. 4 give the discontinuity in  $\mu$  in crossing the vapor pressure curve. For a more extended discussion see our article on nitrogen<sup>6</sup> and Burnett's<sup>11</sup> on carbon dioxide. Since the data on these limit curves are useful, and we can determine them best now from the original records, the cross plots made from Figs. 2 and 3 and used to read the data for Fig. 4 were used again to interpolate curves at pressures of 5, 15, 25, 35, 45, 55, 65 atm. among those in Fig. 4 at 1, 20, 60 and 73 atm. A large scale plot like Fig. 4 was made but with unbroken  $\mu$  and  $t$  scales. The temperatures at which these pressures occur on the vapor pressure curve are the temperatures locating the vertical lines (isothermals) along which the discontinuity in  $\mu$  occurs. The upper and lower section points of each isothermal, with its corresponding pressure isopiestic, give points through which the upper and

lower branches of the limit curve pass. The data for these two series are in Table V. The new large scale drawing is too finely detailed in its active parts to be usefully reproduced, but a few observations about it are pertinent.

The isopiestic (1-65 atm.) all cross each other at close to one point,  $t = 44^\circ$  and  $\mu = 0.93^\circ/\text{atm}$ . In Burnett's diagram<sup>11</sup> (p. 84) the crossing points are not so compacted and they lie approximately at  $t = 15^\circ$  and  $\mu = 1.2^\circ/\text{atm}$ .

Our limit curve differs markedly from his, first in the long, nearly vertical part on both sides of the critical point; second, in the presence of the sharp bend near  $t = 25^\circ$  and  $\mu = 1.15/\text{atm}$ ; third, in the nearness of the inversion in curvature to this bend; and fourth, in the more concentrated curvature in the lower branch. He follows the lower branch farther and we follow the upper. He made a surprisingly good formulation from his rather meager data. Our curve is founded more directly on more numerous and more reliable data.

The values of  $\mu$  for a series of integer values of  $t$  and  $p$  were read off from the large scale plot of Fig. 4 and are given in Table VI. Because of the complexity in the behavior of  $\mu$  about the critical state, it is necessary, for usefulness, to put in many different temperatures in this region.

**Inversion Curve ( $\mu = 0$ ).**—The isopiestic in Fig. 4 cross the line for  $\mu = 0$  at the low temperature side of the diagram. The pressures and temperatures of these points have been read off the precise plots and are given in Table VII. They are plotted in both Figs. 2 and 3, thus giving the

TABLE V  
DATE FOR LIQUID AND VAPOR LIMIT CURVE IN FIG. 4

$t, ^\circ\text{C.}$	$p, \text{atm.}$	lower $\mu$ branch (liquid)	upper $\mu$ branch (vapor)
31	73.0	0.605	0.605
30	71.2	.315	1.010
25	63.5	.201	1.161
20	56.5	.158	1.225
10	44.4	.099	1.341
0	34.4	.058	1.490
-10	26.1	.028	1.659
-20	19.4	.008	1.842
-30	14.1	-.003	2.072
-40	9.9	-.011	2.44
-50	6.7	-.014	

TABLE VI

$\mu$ AS A FUNCTION OF $t$ AND $p$		20	60	73	100	140	180	200	
$t, ^\circ\text{C.}$	$p, \text{atm.}$	1	20	60	73	100	140	180	200
300	0.2650	0.2425	0.2080	0.2002	0.1872	0.1700	0.1540	0.1505	
250	.3075	.2885	.2625	.2565	.2420	.2235	.2045	.1975	
200	.3770	.3575	.3400	.3325	.3150	.2890	.2600	.2455	
150	.4890	.4695	.4430	.4380	.4155	.3760	.3102	.2910	
125	.5600	.5450	.5160	.5068	.4750	.4130	.3230	.2915	
100	.6490	.6375	.6080	.5920	.5405	.4320	.3000	.2555	
90	.6900	.6785	.6500	.6300	.5680	.4290	.2738	.2300	
80	.7350	.7240	.6955	.6725	.5973	.4050	.2343	.1960	
70	.7855	.7750	.7465	.7175	.6192	.3505	.1875	.1600	
60	.8375	.8325	.8060	.7675	.6250	.2625	.1405	.1245	
50	.8950	.8950	.8800	.8225	.5570	.1720	.1025	.0930	
40	.9575	.9655	.9705	.8760	.2620	.1075	.0723	.0660	
30	1.0265	1.0430	1.0835	.2870	.1215	.0678	.0495	.0445	
20	1.1050	1.1355	0.1435	.1075	.0700	.0420	.0320	.0272	
10	1.1910	1.2520	.0720	.0578	.0407	.0235	.0182	.0142	
0	1.2900	1.4020	.0370	.0310	.0215	.0115	.0085	.0045	
-25	1.6500	0.0000	-.0028	-.0030	-.0050	-.0062	-.0080	-.0115	
-50	2.4130	-.0140	-.0150	-.0165	-.0160	-.0183	-.0228	-.0248	
-75		-.0200	-.0200	-.0232	-.0228	-0.240	-.0250	-.0290	

TABLE VII  
DATA FOR THE LOWER BRANCH OF THE INVERSION CURVE  
( $\mu = 0$ )

$p$ , atm.	$-t$ , °C.
20	24.5
60	22.3
73	21.8
100	18.2
140	13.5
180	11.3
200	7.1

lower branch of the inversion curve. This curve seems unusually far below the critical temperature, but calculation shows that in terms of reduced temperatures it is closely the same as that of nitrogen and of argon. Also, estimates from the nitrogen data on the basis of the theorem of corresponding states indicate that the upper branch of the inversion curve for carbon dioxide crosses the  $p = 1$  atm. line at  $1226^\circ$ , so that the whole upper branch is well beyond our facilities.

Burnett as well as Jenkin and Pye observed this inversion of the Joule-Thomson effect in liquid carbon dioxide. Burnett<sup>11</sup> places it at "about  $-24^\circ$ ."

**General Thermodynamic Properties.**—It was intended to combine these experimental data with data on  $pv$  and  $C_p$  from the literature to obtain the series of thermodynamic coefficients for carbon dioxide as was done for air and helium. The literature yielded sufficient coherent  $pv$  data for this purpose, but only insufficient, fragmentary and incoherent data on  $C_p$ . Since  $\Delta h = C_p \Delta t$  is constant between any pair of isenthalps, it is possible to spread  $C_p$  over the whole field if it is known at any constant pressure, preferably above  $p_c$ , over the temperature range. Jenkin and Shorthose<sup>19</sup> give some total heat (enthalpy) data from which one can calculate  $C_p = (\Delta h / \Delta t)_p$ , for part of our field. However, the data consist of rather widely spaced points with their inevitable experimental uncertainty. Moreover, in the neighborhood of the vapor pressure curve—the region with which the work here is chiefly concerned—these enthalpy-temperature isopiestic all have inflection points. Hence the slopes of these curves in our region could not be determined

(19) Jenkin and Shorthose, *Proc. Roy. Soc. (London)*, **A99**, 352 (1921).

with an accuracy sufficient for our purpose, and the attempt to use them was abandoned.

The  $C_p$  data listed by Quinn and Jones<sup>9</sup> either fall outside the field in which we need them, or their original derivation appears so uncertain as to make them of dubious value. Plank and Kuprianoff<sup>18</sup> in the discussion of the source data for their engineering temperature-entropy diagram admit the considerable uncertainty involved. The simplest experimental solution seems to be to measure the relative specific heats along an isopiestic above  $p_c$  over the temperature range.

It is a pleasure to acknowledge our indebtedness to the Wisconsin Alumni Research Foundation for their generous grant allowing support of two part-time workers. We are also indebted to the Rumford Fund of the American Academy of Arts and Sciences, part of whose grant was used for the provision of necessary supplies; to the Works Progress Administration who provided funds for the support of an assistant over the summer of 1939; to the National Youth Administration whose funds provided a helper, M. M. Vance, who did a considerable share of the calculation required for the preparation of the data; and to Dr. Harold Osterberg, who helped make the necessary modifications in the previous apparatus and who assisted in taking the first of the data.

### Summary

1. A large group of isenthalpic curves lying between  $-55$  and  $300^\circ$  and between 1 and 200 atm. have been measured with carbon dioxide. Special care has been given to the region in the neighborhood of the vapor pressure curve and the critical state.

2. The Joule-Thomson coefficient has been calculated from these measurements for the whole field and tabulated as a function of the temperature at a series of constant pressures.

3. Carbon dioxide was almost completely freed of volatile impurity (air) by freezing the liquid ( $-80^\circ$ ) and purging the vapor phase.

4. The inversion curve in the liquid region has been located, as well as the contact point (tangency) of a particular isenthalp with the vapor pressure curve.